Modeling Study of Atmospheric Boundary Layer Characteristics in Industrial City by the Example of Chelyabinsk

Lenskaya Olga Yu.*, Sanjar M. Abdullaev*
*South Ural State University

1. Introduction

Urbanization considerably modifies local and regional atmospheric properties, first of all planetary boundary layer structure, by perturbing the wind, temperature, moisture, turbulence, and surface energy budget fields. The numerical weather modelling is widely used for the urbanized territories. Obviously local circulations studies will be actual for majority of large cities of Russia with polluted atmospheric air and, in particular, for Chelyabinsk combining historically the role of regional megalopolis and the largest industrial center (Abdullaev et al, 2008; Korableva, Lenskaya 2010). In this work the mesoscale numerical WRF model (Weather Research and Forecasting) is used for study of general characteristics of urban heat island and boundary layer structure over the territory of Chelyabinsk.

To investigate local weather phenomena WRF model v 3.4 (Skamarock, 2008) was installed in 2012 in Supercomputer Simulation Laboratory of South Ural State University (Chelyabinsk) on "Tornado SUSU" Supercomputer http://supercomputer.susu.ac.ru/en/computers/tornado/

2. Data and methods

In order to study urban boundary layer characteristics over Chelyabinsk metropolitan area we combine some instrumental observations and the coupled WRF/Noah/UCM model to define, in the first place, the horizontal and vertical configuration of Urban Heat Island during winter anticyclonic weather. These weather conditions are favorable for thermal inversion development and raise the atmosphere pollution in industrial city We integrate the Advanced Research WRF (version 3.4) over single domain shown in Fig. 1.
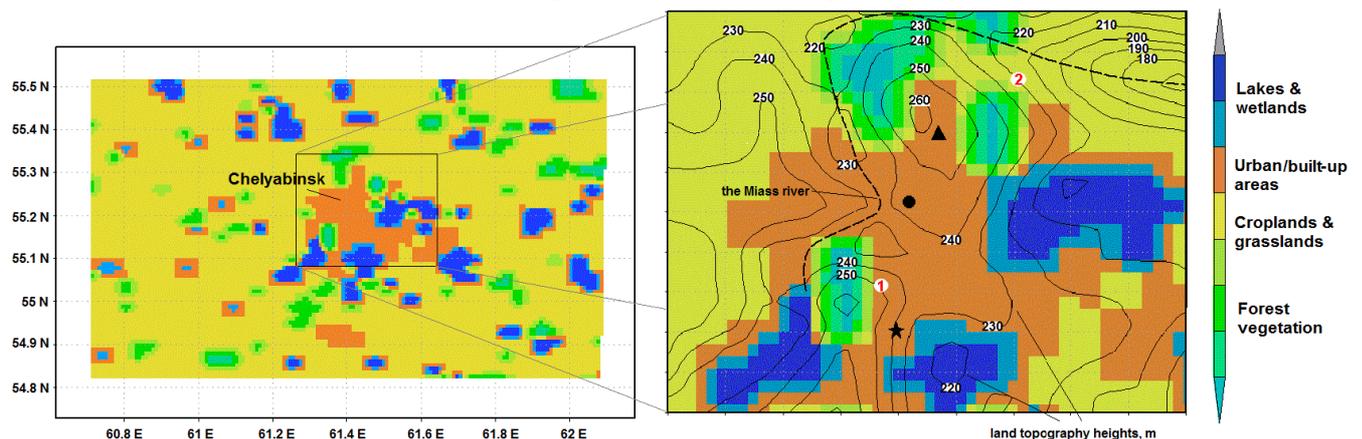

Figure 1. Area of application. 1- meteorological profiler, 2 – weather station

The grid spacing (grid numbers) of this domain is 2 km (45 × 40). The vertical grid contains 35 sigma levels from the surface to 50 hPa, of which the lowest 7 levels are below 1 km so as to have finer resolution in the PBL. A 48-h simulation (0600 LST 08 December – 0600 LST 10 December 2011) is conducted with the initial and boundary conditions from NCEP operational Global Final (FNL) Analyses on a 0.5°×0.5° grid. We use the Yonsei University scheme PBL scheme. Other physical parameterizations include the WRF single-moment 3-class scheme, the shortwave radiation Dudhia schemes, the Rapid Radiative Transfer Model longwave radiation scheme, and the Noah land surface model. Surface-layer physics option: Monin–Obukhov scheme; for urban surface Urban canopy model: 3-category UCM option with surface effects for roofs, walls and streets. To take into account frozen lake areas the static data set landuse_30s_with_lakes was used.

3. Model Evaluation against Observation

The main objectives of the study included testing of planetary boundary layer simulation quality during specific conditions of steady weather. First of all it was necessary to be convinced that the chosen configuration of model well describes temporal changes in boundary layer characteristics. For this purpose hourly output products of model were compared with observed smoothed temperature and wind series, at 2 m above the ground on the surface station and with data of microwave temperature profiler in other place of the city (Fig. 1).

3.1 Evolution of boundary layer parameters

WRF predictions are in good accordance with measurements at the weather station located in the site just north of Chelyabinsk. Comparison of temporal series modelling t_m and observed t_o showed that the model

significantly smoothes the daily fluctuations amplitude of temperature really observed. Absolute difference of temperature and wind speed decreases as the model run. The 48 h average values of temperature and wind speed are close to each other:

$$t_m = -15.3 \pm 1.4^{\circ}C \; ; \; t_o = -14.1 \pm 2.7^{\circ}C \; ; \; ws_m = 1.7 \pm 1 \; m/s \; ; \; ws_0 = 2.0 \pm 1.6 \; m/s$$

Average wind speed at station, $V_o = 2.0 \pm 1.6$ m/s also exceed the modelled $V_m = 1.7 \pm 1$ m/s, but in this case wind speed difference ΔV is decreased during observation in an obvious consent with a temporal changes of temperature difference Δt (fig. 2).
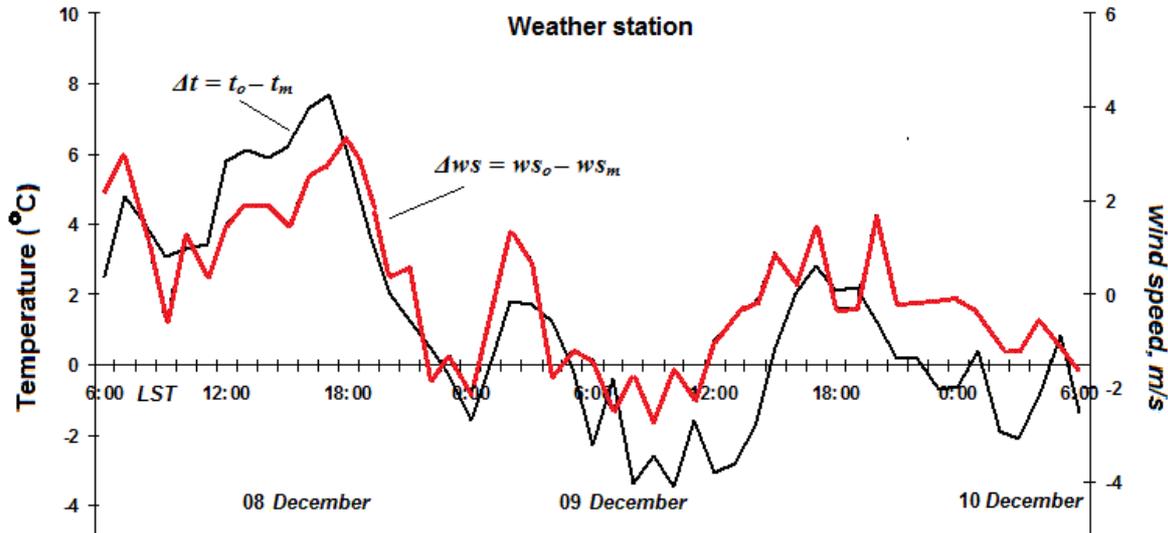

Figure 2. Air temperature and wind speed time series difference as calculated by WRF at 2 m (t_m , ws_m) and as measured (t_0 , ws_0)

Comparison of observed and modelled sea level pressure shows (the figure not produced here) that within the first 18 hours of simulation there was obvious "adaptation" of model to initial and boundary conditions. So hereinafter we focus attention on time interval from 00:00 on December 09 when the modeling results could be considered as steady.

Evolution of observed and modelled temperature in boundary layer at some levels was considered also. As one would expect, at the nearest to a ground level 70 m the temperature amplitude as t_o, and t_m is higher then the upper levels. Above, at levels of 264 m and 402 m the range of Δt is 2-3°C more, than on the ground layer, and the smallest modules of Δt are observed on 155 m.
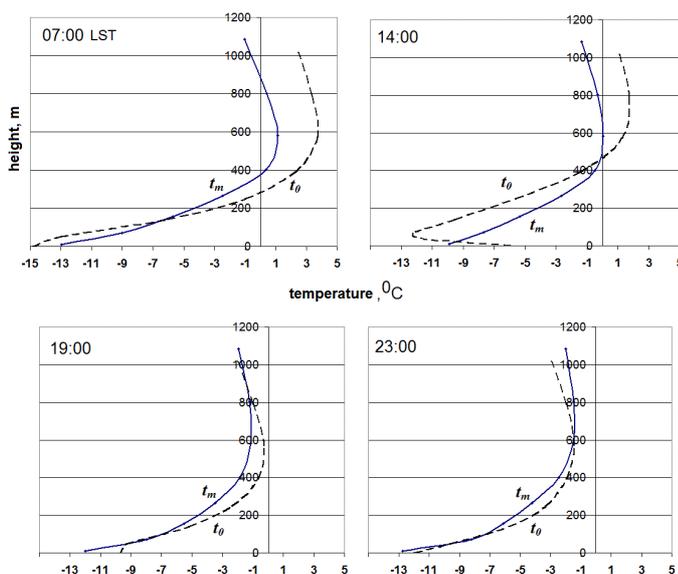
Note that termal stratification (fig. 3) of $t_m(z)$ reproduced by model significantly differs from observed $t_o(z)$. When the difference Δt is minimal, comparing morning (07:00) and day (14:00) stratification at 9 December, note that model significantly smoothes temperature contrast between the bottom and top of boundary layer, i.e. actually underestimates the intensity of inversion. The $t_m(z)$ and $t_o(z)$ difference is more evident during morning and daytime, less in the evening (19:00, 23:00). Maximum deviations Δt are observed exactly during the temperature increase.

Thus, the cold anticyclone weather boundary layer thermal inversion is captured as by WRF and observation. Calculated temperature profile is more smoothed probably due to inadequate static data resolution and therefore UCM used. The difference is most pronounced in the morning.

Figure 3. Boundary layer thermal stratification as calculated by WRF t_m and as measured by MTP-5 t_0

3.2 Time – spatial distribution of UHI characteristics

Within the city the Miass River valley divides heat island on western and eastern parts. Fig. 4 shows the modeling air temperature anomaly of 2 m heihgt relatively mean temperature over area of application at 7 and 14 h 9 Dec 2011. At night and the early morning (fig. 4 left) when temperatures are minimum, the intensity of heat island is maximum. The contrast between temperature in the city and suburban territories reaches 3.5 °C and differs on a square of the city. The greatest contrasts correspond to large industrial and transport zones and central areas. In the afternoon (fig. 4 right), contrast remains, but its intensity decreases to 2°C in the southern part of the city.
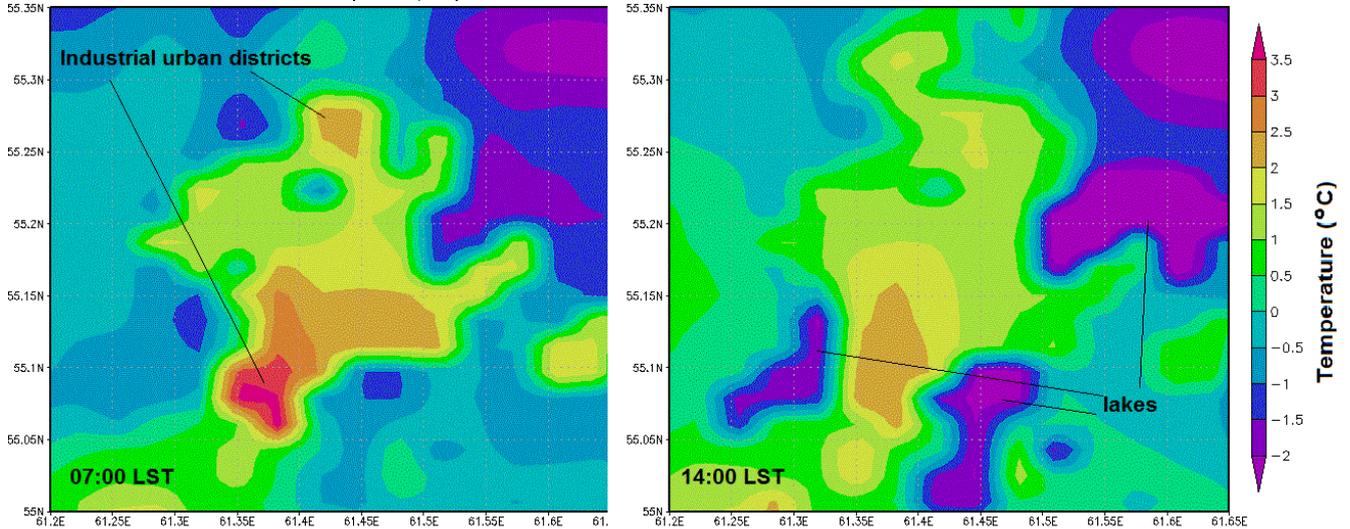

Figure 4. Modeling air temperature anomaly of 2 m heihgt relatively mean temperature over area of application at 7 and 14 h LST 9 Dec 2011

A form and horizontal extent of UHI isotherms in boundary layer were investigated during the warming up and maximum anthropogenous heat emissions in 16 h LST on December 9 (fig. 5a), and also at night 00 h LST on December 10 (fig. 5b). During simulation period 8 – 10 Dec 2011 the canopy layer over river valley remains cooler 1-2°C than surrounding higher building up and industrial areas. So, the UHI of Chelyabinsk is devided in two parts by river valley and is more enhenced early in the morning (in winter)/

3.3 UHI circulations

The simulation of air circulation reveals that at 7 h LST pronounced convergence zones (dark blue in Fig. 6a) coinside with river valley and frozen lakes where cold and more dense air outlet is present. Their coincidence to the Miass River valley, Smolino's lake and other negative forms of a relief (fig. 6a, at the left) it is possible to interpret that in the conditions of steady anti-cyclonic weather night cooling of a terrestrial surface promotes a drain of cold air from heights to lowlands. Over central part of the city and especially over the sublime industrial territory there are winds divergence exceeding $5 \cdot 10^{-4}$ c^{-1}. At the height of 90 m over a surface the divergence decreases to $3 \cdot 10^{-4}$ c^{-1} remaining in the same place.

In fig. 6b stream lines and the position of divergence and convergence zones are shown. Stream lines are built in such a way that the average stream was subtracted from value of wind speed in each point of considered area at this height level. This allows us to reveal the influence of orography
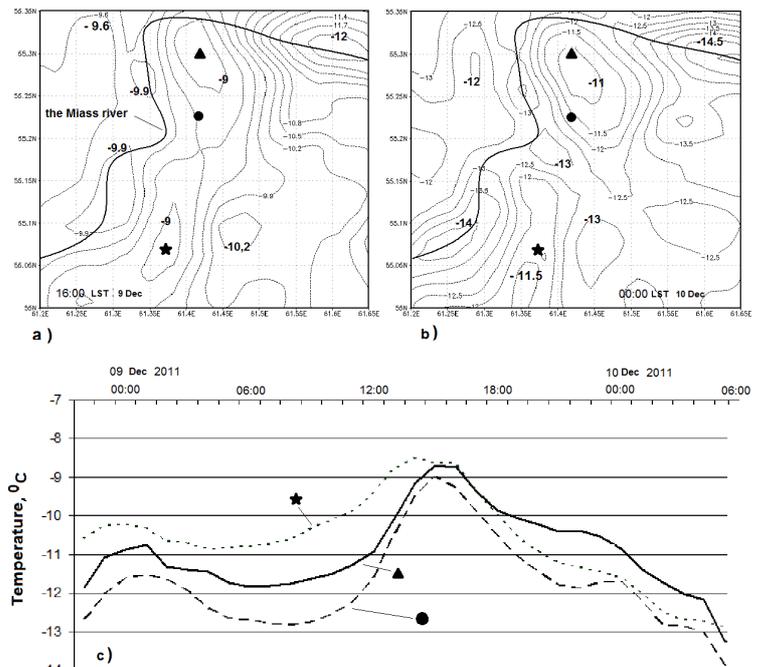

Figure 5. Air temperature field at 70 m above the ground in midafternoon (a) and midnight (b). Air temperature time series in different urban sites (c): highland industrial districts (asterisk and triangle) and river valley (circle)

in residential area and industrial zone on the direction and circulation origin. Stream lines at Fig. 6b reflect the influence of city and its surrounding on air circulation: the divergence above metallurgical urban district at the north and the convergence in the south where there are three frozen lakes.
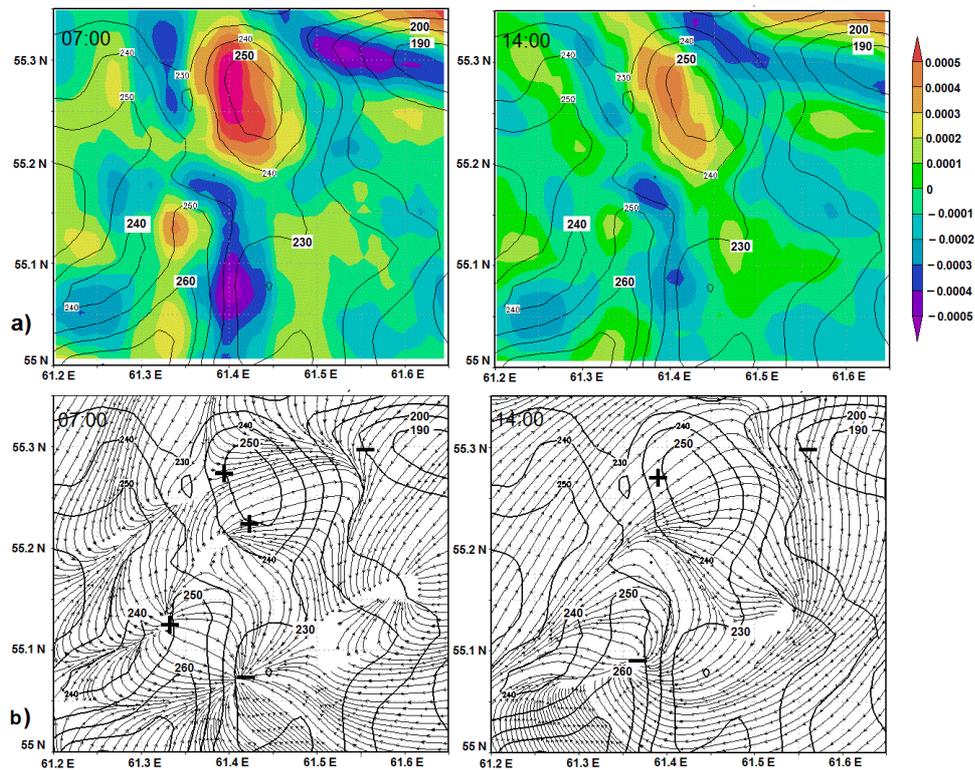

Figure 6. (a) The simulation of divergence field (s^{-1}) at 07 and 14 h LST 30 m above the ground. (b) The wind stream lines at 90 m; the position of positive and negative divergence is shown. Solid lines – topography heights (m).
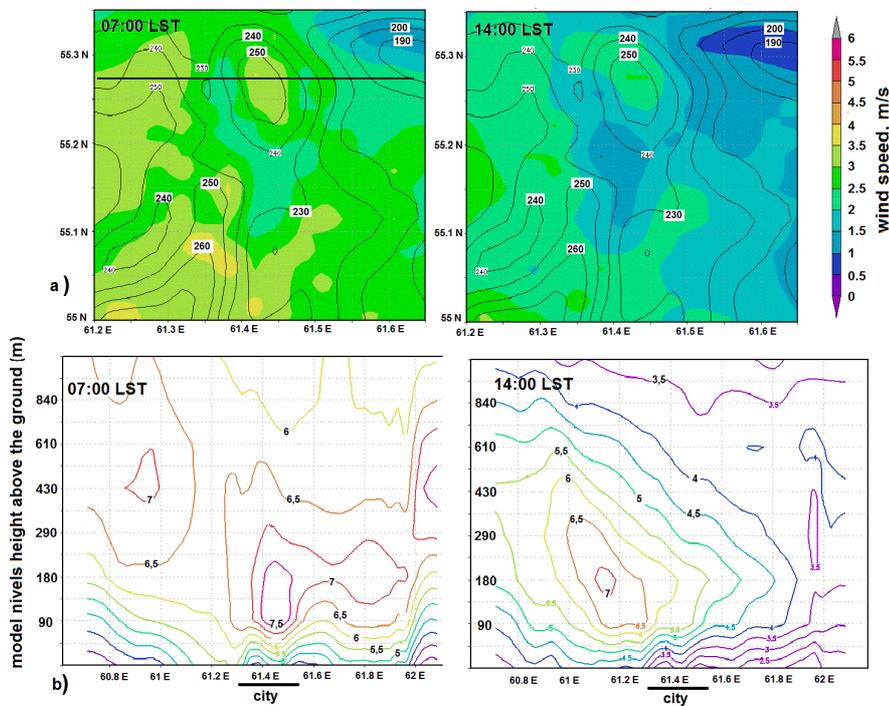

Figure 7. (a) Wind speed distribution (at 10 m) over the city and surrounding; solid lines – land topography heights. (b) Vertical cross section along 55.27 N (black line) of wind speed

During 8 – 10 Dec 2011 wind direction from SW was observed. So the city acts as mesoscale roughness; wind speed decrises to 14:00 LST due to mixing (Fig.7 a). Analysis of temperature gradients, position of

convergence zones and especially character of stream lines in leeward of the city reveal a certain similarity of the mesoscale stationary front with warm air flow on a cold pool and considerable ground gradients of temperature and humidity.

The following found phenomenon can serve one of hypothetical elements of circulation of this front. Wind speed cross section above metallurgical industrial district detects the jet achieving 7.5 m/s at the top of canopy layer (Fig.7 b). In the afternoon the horizontal sizes increase, and its intensity weakens. Obviously, the reasons of emergence of such stream can be connected with a flow of an air obstacle and lifting of warm air created by powerful thermal sources of an industrial zone.

Conclusion

The experiment given above on use of WRF system for simulation of urban heat island, can be a positive example of express validation of model in conditions of the limited meteoinformation typical for large russian city.

The WRF/Noah/UCM simulations satisfactorily depict the UHI of Chelyabinsk in winter anticyclone weather conditions. In spite of small altitude differences the relief forms affect the UHI configuration. It was revealed that temperature contrast is more enhenced during early in the morning.

The doublet structure of positive and negative divergence in surface wind fields was observed. And in certain synoptic conditions model simulation reveals the jet at the top of canopy layer above metallurgical urban district.

 Obviously the detailed assessment of local circulation influence on the urbanized environment of South Ural will require further efforts on development of monitoring systems and numerical modeling.

Acknowledgments

References

1. Abdullaev, S.M. Life cycle assessment of nature – anthropogenic systems / S.M. Abdullaev, E.G. Korableva, Y.A. Sapeltseva & Co-authors // Bulletin of Chelyabinsk State University. Serie: Ecology. Environmental Management. – 2008. – Vol. 3. – n 17. – P. 34-45.

2. Skamarock, W.C. A Description of the Advanced Research WRF Version 3. – NCAR Tech. Note, June 2008 / W.C. Skamarock. URL: http://www.mmm.ucar.edu/wrf/users/docs (assess at: 11.01.2013).

3. Korableva, E.G. Chelyabinsk winter Urban Heat Island study / E.G. Korableva, O.Y. Lenskaya // Bulletin of Chelyabinsk State University. Serie: Ecology. Environmental Management.. – 2010. – Vol. 4. – n 8. – P. 15-23.